Bull. Mater. Sci., Vol. 23, No. 3, June 2000, pp. 169–173. © Indian Academy of Sciences.

$La_{0\cdot 9}Sr_{0\cdot 1}Ga_{0\cdot 8}M_{0\cdot 2}O_{3-d}$ (M = Mn, Co, Ni, Cu or Zn): Transition metal-substituted derivatives of lanthanum–strontium–gallium–magnesium (LSGM) perovskite oxide ion conductor

LITTY SEBASTIAN, A K SHUKLA and J GOPALAKRISHNAN*
Solid State and Structural Chemistry Unit, Indian Institute of Science, Bangalore 560 012, India

MS received 10 March 2000

Abstract. **Perovskite oxides of the general formula, $La_{0\cdot 9}Sr_{0\cdot 1}Ga_{0\cdot 8}M_{0\cdot 2}O_{3-d}$ for M = Mn, Co, Ni, Cu and Zn, have been prepared and investigated. All the oxides exhibit high electrical conductivities ($s \sim 10^{-2}$ S/cm at 800°C) comparable to that of the best perovskite oxide ion conductor, $La_{0\cdot 9}Sr_{0\cdot 1}Ga_{0\cdot 8}Mg_{0\cdot 2}O_{2\cdot 85}$ (LSGM) ($s \sim 8 \times 10^{-2}$ S/cm at 800°C). While M = Mn, Co, Ni, Cu members appear to be mixed conductors with a variable electronic contribution to the conductivity, especially at high oxygen partial pressures ($pO_2 \geq 1$ atm), arising from mixed-valency of the transition metals, the M = Zn(II) phase is a pure oxide ion conductor exhibiting a conductivity ($s \sim 1\cdot 5 \times 10^{-2}$ S/cm at 800°C) that is slightly lower than that of LSGM. The lower conductivity of the M = Zn(II) derivative could be due to the preference of Zn(II) for a tetrahedral oxygen coordination.**

Keywords. **LSGM substitution; mixed ionic–electronic conductors; oxide ion conductor.**

1. Introduction

Oxide ion conductors are important materials for application in solid oxide fuel cells (SOFCs), oxygen sensors and oxygen pumps (Goodenough *et al* 1992; Steele 1992; Kendall *et al* 1995; Boivin and Mairesse 1998). Recently, a high oxide ion conductivity ($s = 0\cdot 08$ S/cm 800°C) has been reported for the Sr- and Mg-doped $LaGaO_3$ perovskite of the composition, $La_{0\cdot 9}Sr_{0\cdot 1}Ga_{0\cdot 8}M_{0\cdot 2}O_{2\cdot 85}$ (LSGM) (Feng and Goodenough 1994; Ishihara *et al* 1994; Huang and Petric 1996). This material exhibits a high oxide ion conduction over a broad range of oxygen partial pressures (1–10^{-22} atm) and therefore, it is a promising candidate to replace yttria stabilized zirconia (YSZ) as an electrolyte material in SOFCs operating at relatively low temperatures (600–800°C) (Ishihara *et al* 1996; Huang *et al* 1998).

Compositional modifications at the B site of the perovskite LSGM are likely to influence the nature of the electrical conduction in this material. Thus, substitution of Cr and Fe in $La_{0\cdot 9}Sr_{0\cdot 1}GaO_3$ results in mixed (ionic + electronic) conduction (Baker *et al* 1998). Such mixed conducting materials are attractive as dense ceramic membranes for separation of oxygen from air (Ziehfreund and Maier 1996) and for syn–gas (CO/H_2) production directly from methane (Ishihara *et al* 1995).

In an earlier investigation, we showed that isovalent substitution of Mn(II) for Mg(II) in LSGM yielded a new oxide ion conductor with a conductivity of $4\cdot 6 \times 10^{-2}$ S/cm at 800°C (Thangadurai *et al* 1998). In this work, we have synthesized and investigated transition metal-substituted derivatives of LSGM of the formula, $La_{0\cdot 9}Sr_{0\cdot 1}Ga_{0\cdot 8}M_{0\cdot 2}O_{3-d}$ for M = Co, Ni, Cu and Zn, together with Mn. Members for M = Mn, Co, Ni and Cu containing mixed-valent M(II)/M(III) are mixed conductors, while the M = Zn member is a pure ionic conductor albeit with an ionic conductivity ($s \sim 1\cdot 5 \times 10^{-2}$ S/cm at 800°C) that is slightly lower than that of the LSGM ($s \sim 8 \times 10^{-2}$ S/cm at 800°C). Recently, the effect of additional doping of transition metals at the Ga site to form $La_{0\cdot 9}Sr_{0\cdot 1}(Ga_{1-y}M_y)_{0\cdot 8}Mg_{0\cdot 2}O_{3-x}$ (M = Cr, Mn, Fe and Co) was reported (Trofimenko and Ullmann 1999).

2. Experimental

$La_{0\cdot 9}Sr_{0\cdot 1}Ga_{0\cdot 8}M_{0\cdot 2}O_{3-d}$ (M = Mn, Co, Ni, Cu and Zn) were prepared by heating stoichiometric amounts of La_2O_3 (preheated at 900°C for 12 h), $SrCO_3$, $MC_2O_4\cdot 2H_2O$ (M = Mn, Co, Ni)/MO (M = Cu, Zn) and Ga_2O_3 at 1100°C for 12 h and 1300°C for 12 h in air with intermediate grinding and pelletizing. Oxidation state of the transition metal ions was determined by titrimetry using Fe(II)–$KMnO_4$ solutions. Powder X-ray diffraction (XRD) patterns were recorded on a Siemens D5005 diffractometer using CuK_a radiation. The microstructures of M = Ni, Zn phases were observed with a JEOL JSM–840A scanning electron microscope (SEM). Infrared spectra of the samples were recorded at room temperature with a Perkin Elmer

---

*Author for correspondence

Spectrum 1000 FT-Spectrometer in the spectral region 1000–350 cm^{-1}.

Electrical conductivity was measured on sintered pellets (coated with gold paste, cured at 600°C for 6 h) using HP4194A Impedance/Gain–Phase Analyzer over a frequency range of 100 Hz–15 MHz in the temperature range of 100–800°C. The electrical conductivity measurements were made for at least two heating and cooling cycles. Samples were equilibrated for about 45 min prior to each set of impedance measurements. At low temperatures, the impedance plots of $La_{0\cdot9}Sr_{0\cdot1}Ga_{0\cdot8}Zn_{0\cdot2}O_{3-d}$, could be resolved into two semicircles corresponding to the bulk and grain boundary contributions to the resistivity (Bauerle 1969). Since the bulk and grain boundary semicircles were distinct, we could obtain the bulk conductivity from the semicircle on the high frequency side. Oxygen partial pressure dependence of the conductivity of the samples was investigated at four partial pressures (1, 0·25, 10^{-8} and 10^{-10} atm) at 800°C.

3. Results and discussion

Figure 1 shows powder X-ray diffraction patterns of $La_{0\cdot9}Sr_{0\cdot1}Ga_{0\cdot8}M_{0\cdot2}O_{3-d}$ (M = Mn, Co, Ni, Cu and Zn). All the phases adopt perovskite type structures similar to LSGM (Slater *et al* 1998a, b). For M = Mn, we see a weak reflection at $d = 2\cdot98$ Å due to La_4SrO_7 impurity, while for M = Zn, we see a weak reflection at $d = 2\cdot84$ Å which is likely due to $LaSrGaO_4$ impurity. All other $La_{0\cdot9}Sr_{0\cdot1}Ga_{0\cdot8}M_{0\cdot2}O_{3-d}$ are single-phase perovskite materials. The crystal systems, oxygen content, lattice parameters, and unit cell volumes per formula unit along with the conductivity data of these compounds are summarized in table 1. We see a rhombohedral distortion from the ideal cubic structure for M = Mn, Ni and Co, while the M = Zn phase shows the formation of a cubic perovskite with $a = 3\cdot898$ Å. The M = Cu phase could be indexed on an orthorhombic system ($GdFeO_3$ type structure) similar to that of the parent $LaGaO_3$ phase. The powder XRD data for $La_{0\cdot9}Sr_{0\cdot1}Ga_{0\cdot8}Ni_{0\cdot2}O_{3-d}$ are indexed in table 2. Oxygen stoichiometry was experimentally determined by ferrous ammonium sulphate titration against standard $KMnO_4$. The *d* values obtained are listed in table 1. It is found that the transition metals exist in the trivalent state in the compounds to an extent of 5–25%.

Electrical conductivity *s* of $La_{0\cdot9}Sr_{0\cdot1}Ga_{0\cdot8}M_{0\cdot2}O_{3-d}$ were obtained from a.c. impedance measurements. The impedance spectra measured in air at 320°C for $La_{0\cdot9}Sr_{0\cdot1}Ga_{0\cdot8}M_{0\cdot2}O_{3-d}$ (M = Co, Zn) are given in figure 2. The typical impedance plots of $La_{0\cdot9}Sr_{0\cdot1}Ga_{0\cdot8}M_{0\cdot2}O_{3-d}$ (M = Mn, Ni and Co) show a perfect semicircle in the lower temperature region, indicating the absence of grain boundary effects. On the other hand, M = Zn phase shows

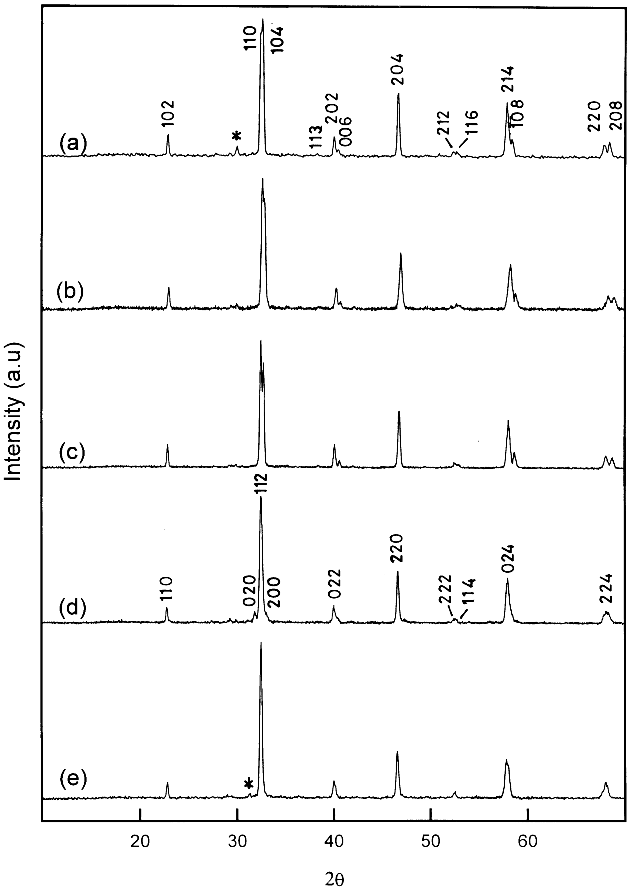

Figure 1. Powder XRD patterns of $La_{0\cdot9}Sr_{0\cdot1}Ga_{0\cdot8}M_{0\cdot2}O_{3-d}$. (a) M = Mn, (b) M = Co, (c) M = Ni, (d) M = Cu and (e) M = Zn. Impurity reflections in (a) and (e) are marked by asterisks.

Table 1. Chemical composition, lattice parameters and electrical conductivity of $La_{0\cdot9}Sr_{0\cdot1}Ga_{0\cdot8}M_{0\cdot2}O_{3-d}$.

Composition	*d*	Structure	*a* (Å)	*b* (Å)	*c* (Å)	Volume per ABO_3 unit cell ($Å^3$)	*s* 800°C (S/cm)	E_a (eV)
$La_{0\cdot9}Sr_{0\cdot1}Ga_{0\cdot8}Mn_{0\cdot2}O_{3-d}$	0·120	Rhombohedral[a]	5·518(1)	–	13·335(4)	58·60	$2\cdot93 \times 10^{-2}$	0·38
$La_{0\cdot9}Sr_{0\cdot1}Ga_{0\cdot8}Co_{0\cdot2}O_{3-d}$	0·130	Rhombohedral[a]	5·494(1)	–	13·298(3)	57·94	$3\cdot98 \times 10^{-2}$	0·44
$La_{0\cdot9}Sr_{0\cdot1}Ga_{0\cdot8}Ni_{0\cdot2}O_{3-d}$	0·145	Rhombohedral[a]	5·513(1)	–	13·320(6)	58·42	$5\cdot66 \times 10^{-2}$	0·43
$La_{0\cdot9}Sr_{0\cdot1}Ga_{0\cdot8}Cu_{0\cdot2}O_{3-d}$	0·130	Orthorhombic	5·417(3)	5·610(4)	7·760(3)	58·97	$1\cdot82 \times 10^{-2}$	0·63
$La_{0\cdot9}Sr_{0\cdot1}Ga_{0\cdot8}Zn_{0\cdot2}O_{3-d}$	0·150	Pseudocubic	3·898(1)	–	–	59·22	$1\cdot49 \times 10^{-2}$	0·79
$La_{0\cdot9}Sr_{0\cdot1}Ga_{0\cdot8}Mg_{0\cdot2}O_{3-d}$	0·150	Monoclinic[b]	–	–	–	59·69	$8\cdot00 \times 10^{-2}$	1·07

[a]hexagonal lattice parameters are given; [b]the lattice parameters are $a = 7\cdot816$, $b = 5\cdot539$, $c = 5\cdot515$ Å, $b = 90\cdot06°$ (Slater *et al* 1998a, b).

Table 2. Powder XRD data for $La_{0.9}Sr_{0.1}Ga_{0.8}Ni_{0.2}O_{3-d}$.

h	*k*	*l*	d_{obs} (Å)	d_{cal} (Å)[a]	I_{obs}
1	0	2	3·890	3·880	21
1	1	0	2·754	2·756	100
1	0	4	2·735	2·731	83
1	1	3	2·344	2·341	5
2	0	2	2·247	2·247	21
0	0	6	2·220	2·219	9
2	0	4	1·940	1·940	46
2	1	2	1·744	1·741	7
1	1	6	1·727	1·728	6
2	1	4	1·587	1·586	35
1	0	8	1·573	1·572	20
2	2	0	1·377	1·378	16
2	0	8	1·364	1·365	10
3	1	4	1·230	1·230	16
2	1	8	1·223	1·223	15

[a] Calculated for the lattice parameters listed in table 1.

a large grain boundary impedance which is likely to be due to the presence of an impurity phase at the grain boundary. This was further evidenced by the SEM images of M = Ni and Zn phases given in figure 3. The Ni phase shows a cleaner grain boundary than the Zn phase.

The Arrhenius plots for the conductivity of $La_{0.9}Sr_{0.1}Ga_{0.8}M_{0.2}O_{3-d}$ are shown in figure 4. The conductivity s at 800°C and the activation energy (E_a) values obtained from the Arrhenius plots are given in table 1. All of them show a conductivity in the same order of magnitude as LSGM ($s \sim 10^{-2}$ S/cm at 800°C). Among the samples investigated, the M = Ni compound exhibits the highest conductivity, s, of $5{\cdot}6 \times 10^{-2}$ S/cm at 800°C with an activation energy of 0·43 eV. This value is comparable to the conductivity of LSGM ($s = 8 \times 10^{-2}$ S/cm at 800°C). The lower activation energies observed could be attributed to the influence of electronic contribution to the conductivity (Baker *et al* 1998; Trofimenko and Ullmann 1999). Among

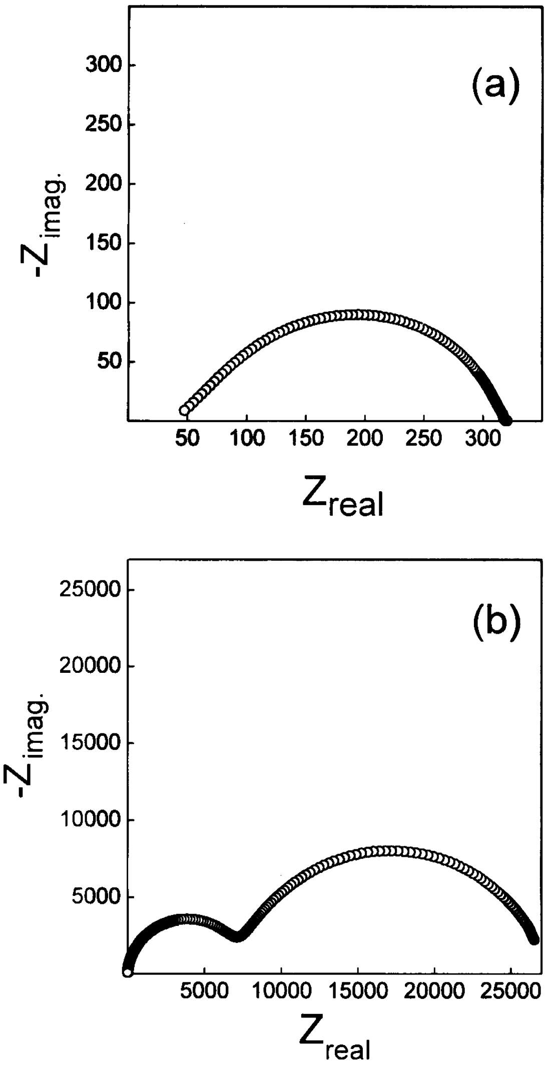

Figure 2. Typical a.c. impedance plots for (**a**) M = Co and (**b**) M = Zn at 320°C.

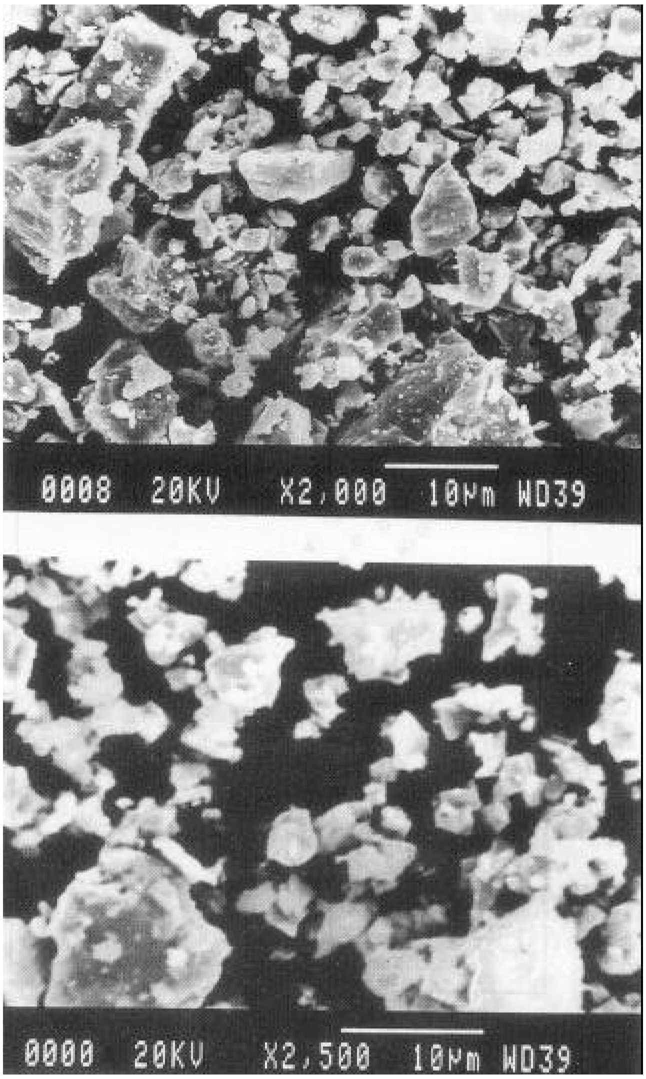

Figure 3. Scanning electron micrographs showing $La_{0.9}Sr_{0.1}Ga_{0.8}M_{0.2}O_{3-d}$ (M = Ni (top) and M = Zn (bottom)).

the LSGM derivatives investigated, we expected the M = Zn phase to show exclusive ionic conductivity comparable to that of the M = Mg (LSGM) phase because Zn(II) is divalent having an ionic radius (r = 0·74 Å) comparable to that of Mg(II) (r = 0·72 Å) (Shannon 1976). The lower conductivity of M = Zn phase could be due to the preference of Zn(II) for tetrahedral oxygen coordination which could result in local trapping of oxide ions around Zn(II). We do see an evidence for a tetrahedral coordination of Zn(II) in the IR spectrum of $La_{0.9}Sr_{0.1}Ga_{0.8}Zn_{0.2}O_{2.85}$. All the LSGM derivatives show two strong absorption bands around 620 and 380 cm^{-1} (figure 5) which are due to Ga(M)–O stretching and O–Ga(M)–O bending, respectively (Yaremehenko *et al* 1999). While the band due to Ga(M)–O stretch is symmetrical in all the LSGM derivatives, it is unsymmetrical in the case of M = Zn(II) showing a distinct shoulder on the high frequency side of the 620 cm^{-1} band (figure 5e). We believe the high frequency shoulder is a clear signature of tetrahedrally coordinated Zn(II). Tetrahedral site Zn(II) is known to show Zn–O stretch vibration around 670 cm^{-1} in metal oxides (Ross 1972).

To determine the nature of electrical conduction, we investigated the oxygen partial pressure dependence of the conductivity. The electrical conductivity of $La_{0.9}Sr_{0.1}Ga_{0.8}M_{0.2}O_{3-d}$ (M = Ni, Co, Cu and Zn) at 800°C as a function of oxygen partial pressure (pO_2) is shown in figure 6. In the case of $La_{0.9}Sr_{0.1}Ga_{0.8}Zn_{0.2}O_{2.85}$, the conductivity was found to be independent of the partial pressure of oxygen in the range 1–10^{-10} atm revealing that the conductivity is purely ionic in origin. Considerable electronic conduction appears at high oxygen partial pressures for M = Mn, Co, Ni and Cu derivatives suggesting p-type electronic contribution to the conductivity.

4. Conclusion

We have prepared 3d-transition metal substituted derivatives of one of the best oxide ion conductors known in the literature, viz. $La_{0.9}Sr_{0.1}Ga_{0.8}Mg_{0.2}O_{2.85}$ (LSGM), by replacing Mg with M = Mn, Co, Ni, Cu or Zn. All of them crystallize with perovskite type structures having a disordered distribution of Ga/M at the octahedral sites. All the members exhibit a high electrical conductivity comparable to that of LSGM. While the conduction in M = Mn, Co, Ni or Cu members is likely to be both ionic and electronic, the M = Zn(II) member is a pure ionic conductor, albeit the conductivity is slightly lower than that of the parent LSGM.

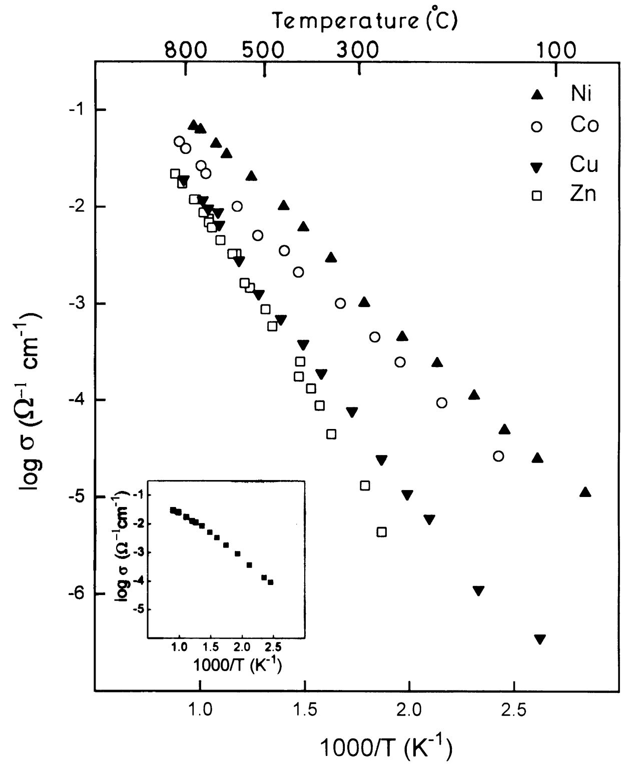

Figure 4. Arrhenius plots for the conductivity of $La_{0.9}Sr_{0.1}Ga_{0.8}M_{0.2}O_{3-d}$ (M = Ni (▲), M = Co (O), M = Cu (▼) and M = Zn (□)). Inset shows the corresponding data for M = Mn (■).

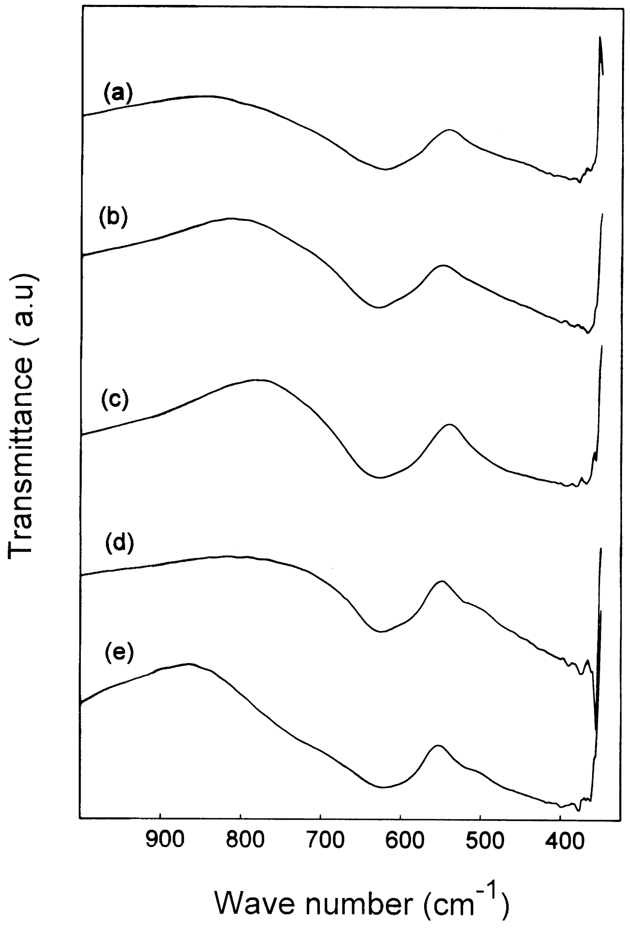

Figure 5. FTIR spectra of $La_{0.9}Sr_{0.1}Ga_{0.8}M_{0.2}O_{3-d}$. (a) M = Mn, (b) M = Co, (c) M = Ni, (d) M = Cu and (e) M = Zn.

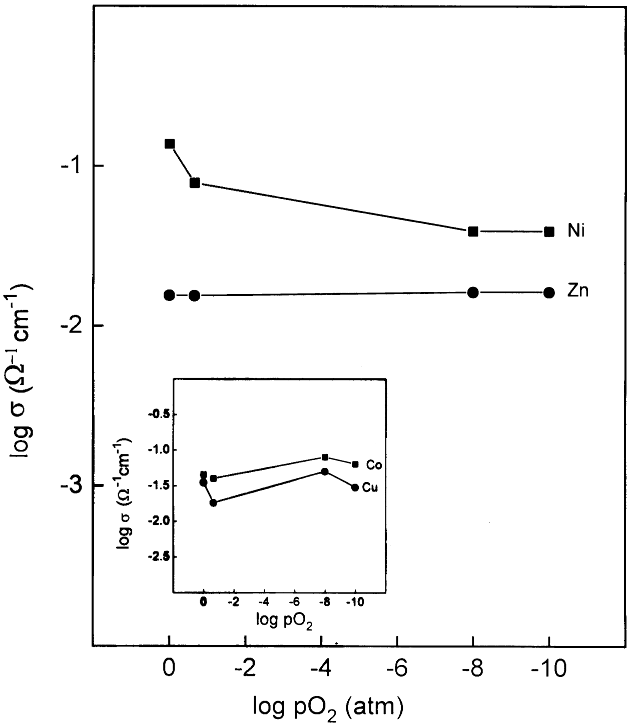

Figure 6. Dependence of electrical conductivity of $La_{0·9}Sr_{0·1}Ga_{0·8}M_{0·2}O_{3-d}$ on oxygen partial pressure at 800°C.

Acknowledgements

We thank Dr V Thangadurai for his help in electrical conductivity measurements. We also thank the Department of Science and Technology, New Delhi for financial support. One of the authors (LS) thanks the Council of Scientific and Industrial Research, New Delhi, for the award of a research fellowship.

References

Baker R T, Gharbage B and Marques F M B 1998 *J. Eur. Ceram. Soc.* **18** 105

Boivin J C and Mairesse G 1998 *Chem. Mater.* **10** 2870

Bauerle J E 1969 *J. Phys. Chem. Solids* **30** 2657

Feng M and Goodenough J B 1994 *Eur. J. Solid State Inorg. Chem.* **31** 663

Goodenough J B, Manthiram A, Paranthaman M and Zhen Y S 1992 *Mater. Sci. and Engg.* **B12** 357

Huang P and Petric A 1996 *J. Electrochem. Soc.* **143** 1644

Huang K, Tichy R, Goodenough J B and Milliken C 1998 *J. Am. Ceram. Soc.* **81** 2581

Ishihara T, Hiei Y and Takita Y 1995 *Solid State Ionics* **79** 371

Ishihara T, Matsuda H and Takita Y 1994 *J. Am. Chem. Soc.* **116** 3801

Ishihara T, Minami H, Matsuda H, Nishiguchi H and Takita Y 1996 *Chem. Commun.* 929

Kendall K R, Navas C, Thomas J K and Zur Loye H C 1995 *Solid State Ionics* **82** 215

Ross S D 1972 in *Inorganic infrared and Raman spectra* (London: McGraw-Hill Book Company (UK) Ltd)

Shannon R D 1976 *Acta Crystallogr.* **A32** 751

Slater P R, Irvine J T S, Ishihara T and Takita Y 1998a *Solid State Ionics* **107** 319

Slater P R, Irvine J T S, Ishihara T and Takita Y 1998b *J. Solid State Chem.* **139** 135

Steele B C H 1992 *Mater. Sci. Engg.* **B13** 79

Thangadurai V, Shukla A K and Gopalakrishnan J 1998 *Chem. Commun.* 2647

Trofimenko N and Ullmann H 1999 *Solid State Ionics* **118** 215

Yaremehenko A A, Kharton V V, Viskup A P, Naumovich E N, Lapchuk N M and Tikhonovich V N 1999 *J. Solid State Chem.* **142** 325

Ziehfreund A and Maier W F 1996 *Chem. Mater.* **8** 2721